Food and Chemical Toxicology 134 (2019) 110803

Contents lists available at ScienceDirect

Food and Chemical Toxicology

journal homepage: www.elsevier.com/locate/foodchemtox

Dioxin-like (DL-) polychlorinated biphenyls induced immunotoxicity through apoptosis in mice splenocytes via the AhR mediated mitochondria dependent signaling pathways

Fang Du[a,1], Ting Zhao[a,*,1], Hong-Chen Ji[a], Ying-Biao Luo[a], Fen Wang[a], Guang-Hua Mao[b], Wei-Wei Feng[b], Yao Chen[b], Xiang-Yang Wu[b], Liu-Qing Yang[a,**]

[a] School of Chemistry and Chemical Engineering, Jiangsu University, Xuefu Rd. 301, Zhenjiang, 212013, China
[b] School of the Environment, Jiangsu University, Xuefu Rd. 301, Zhenjiang, 212013, Jiangsu, China

ARTICLE INFO

Keywords:
Polychlorinated biphenyl
Immunotoxicity
AhR
Oxidative damage
Apoptosis
Cytokines

ABSTRACT

Polychlorinated biphenyls (PCBs) would do serious damage to multiple systems, while coplanar polychlorinated biphenyls, the most toxic member of the family, has been widely taken into consideration. In this study, ICR mice were fed with different doses of PCB126 to explore the underlying molecular mechanisms on immunotoxicity. The results showed that PCB126 caused immunosuppression as evidenced by inhibiting the ratios of thymus and spleen weights, changing the organizational structure and decreasing levels and mRNA expression of TNF-α, IFN-γ and IL-2. PCB126 inhibited the SOD activity and spurred the accumulation of MDA in spleen and thymus. Meanwhile, it also disturbed the Nrf2 signaling pathway as evidenced by up-regulating the mRNA expression of Nrf2 and Keap1. Additionally, a remarkable reduction in the mRNA expression of AhR and enhancement in the mRNA expression of Cyp1 enzymes (Cyp1a1, Cyp1a2 and Cyp1b1) were observed, which increased the ROS levels. PCB126 could increase protein expression of Bax, Caspase-3, Caspase-8 and Caspase-9, while the protein expression of Bcl-2 was decreased. In summary, the results indicated that PCB126 modulated the AhR signaling pathway, which interacted with apoptosis and oxidative stress to induce immunotoxicity, enrich the immunotoxicological mechanisms of PCB126.

1. Introduction

Polychlorinated biphenyls (PCBs) are the ubiquitous pollutants which were widely used for a variety of industrial purposes for several decades before their production was banned in the 1970s. The improper procedures for the disposal of municipal waste, such as incomplete combustion of the waste, represent a well-known source of PCBs (Pirard et al., 2005). To date, despite the production and applying of PCBs have been prohibited decades ago in most countries (Wang et al., 2016), recently quantifiable levels of PCBs are still detectable in multiple environment media, including air (Ampleman et al., 2015), soil (Mertes et al., 2018), water (Baqar et al., 2017), sediments (Syed et al., 2014) and dust (Takahashi et al., 2017). However, because of its lipophilicity and bioaccumulation, food is the main route of PCBs exposure and approximately 90% of human exposure to PCBs originates from foods, especially those of animal origin such as poultry (Rusin et al., 2019), fish (Bodin et al., 2014), meat (Zhang et al., 2015), egg (Hoang et al., 2014), milk and their products (Bertocchi et al., 2015). Overall, PCBs are widely distributed in the environment, foods and feeds, which increases the exposure risk of humans and animals.

PCBs are presented in humans as shown in worldwide bio-monitoring studies (Angerer et al., 2007). PCBs could enter into the body and bind to blood lipids, which are transported to different compartments including the liver, thyroid glands, reproductive organs and brain to induce toxic effects in humans (Chu et al., 2019; Falandysz et al., 2019; Gaum et al., 2016; Ingelido et al., 2017) and animals (Deng et al., 2019b; Fiandanese et al., 2016; Fischer et al., 2008; Maranghi et al., 2013). Currently, some investigations indicated that PCB exposure is associated with immunotoxicity (Weisglas-Kuperus et al., 2000). The epidemiology studies (Stølevik et al., 2013) revealed that prenatal exposure to PCBs could increase the risk of wheeze and susceptibility to infectious diseases in offspring, induce the immune

* Corresponding author.
** Corresponding author.
E-mail addresses: zhaoting@ujs.edu.cn (T. Zhao), yangliuqing@ujs.edu.cn (L.-Q. Yang).
[1] Contributed to this article equally and are co-first authors.

https://doi.org/10.1016/j.fct.2019.110803
Received 16 May 2019; Received in revised form 31 August 2019; Accepted 4 September 2019
Available online 26 September 2019

suppression and alter major lymphocyte subsets in early childhood. Studies of animal models indicated that low and high-dose PCB153 exposure could induce immunosuppression in diabetic mice via reducing the number of splenocytes and CD^{4+} T_H cells, inhibiting T cell proliferation and cytokine formation (Kuiper et al., 2016). Meanwhile, studies of cell model in vitro showed that NDL-PCBs could cause a significant reduction in LPS-activated chemokine synthesis, COX-2 and iNOS synthase expression, and macrophage endocytic capacity by disrupting the TLR-4/NF-KB pathway (Santoro et al., 2015).

As we all know, aryl hydrocarbon receptor (AhR) is a cytosolic sensor for various chemicals, such as 2, 3, 7, 8-tetrachlorodibenzo-p-dioxin (TCDD) and polychlorinated biphenyls (PCBs) (Tsuji et al., 2012). For example, TCDD induced neurotoxic effects via AhR activating and up-regulating protein expression of caspase-3 (a key effector caspase in the apoptotic cascade) to induce apoptosis or necrosis (Moraleshernández et al., 2016). In contrast, TCDD also could cause a significant elevation cell apoptosis in $AhR^{-/-}$ model via inhibiting cell survival, and increasing oxidative stress and percentage of caspase-3-positive cells (Marlowe et al., 2008). Importantly, dioxin-like 3, 3′, 4, 4′, 5-pentachlorobiphenyl (PCB 126) had the high affinity to AhR and its value of toxic equivalency factor (TEF) is 0.1 (one-tenth of that for TCDD). For example, PCB126 could up-regulate the mRNA expression of Cyp1a1 and Nrf2 to induce macrophage polarization and inflammation, which indicated PCB126 can disturb immune reaction via AhR mediated pathway (Wang et al., 2019). However, Non-coplanar PCBs (such as PCB 20, 52, 56) enhance the genotoxicity of AFB1 through significantly decreases the protein level of AhR and increases the protein expression of Cyp1a1, Cyp1a2, and Cyp3a4 (Chen and Liu, 2019). In addition, Aroclor1254 and PCB153 could cause immunosuppression by inducing DNA fragmentation and increasing caspase-3 activity in murine spleen cell (Jeon et al., 2002). NDL-PCBs induced chondrocytes apoptosis through depletion of cell viability and Bcl-2/Bax ratio and up-regulation of p38 phosphorylation and caspase-3 expression (Abella et al., 2015). Given the discovery mentioned above, it was concluded that PCBs induce bio-toxicity via the AhR pathway and apoptosis relative pathway.

PCB126 is one of the most prevalent and toxic polychlorinated biphenyls and can exert adverse effects on multiple systems. However, the toxicity on immunotoxicity and mechanism of PCB126 has not been reported. We hypothesized that PCB126 may promote mouse immunotoxicity through AhR-dependent pathway of apoptosis. Therefore, we have investigated the effect of organ indexes, histopathology, ROS level and cytokine secretion to reveal immunotoxicity of PCB126. The induction of the mRNA expression of AhR, Cyp1, Nrf2 and expression of apoptosis-related proteins to provide a further understanding of immunotoxicity mechanism of PCB126.

2. Materials and methods

2.1. Materials

Assay kits for tumor necrosis factor-alpha (TNF-α), interferon-γ (IFN-γ) and interleukin-2 (IL-2) were all obtained from Hefei Bo Mei Bioengineering Institute (Hefei, Anhui Province, China). Assay kits for Maleic dialdehyde (MDA), Superoxide dismutase (SOD) and Reactive oxygen species (ROS) were all obtained from Nanjing Jian Cheng Bioengineering Institute (Nanjing, Jiangsu Province, China). Both total protein extraction and BCA kits were purchased from Beyotime Biotechnology Research Institute (Shanghai, China). All other chemicals and solvents used were of analytical reagent grade and obtained from Sinopharm Chemical Reagent Co., Ltd. (Shanghai, China).

2.2. Animals and experimental setup

ICR mice (18–22 g) were obtained from the Comparative Medicine Center in Yangzhou University, China (the license number SCXK (SU) 2007–0001). After acclimatization for 2–3 days, the mice (half were males and the other females) were housed in standard cages, 28 individuals/cage as one group, with wood shavings as bedding. All of the mice had free access to food and water. The caged mice were maintained under a 12:12-h light-to-dark cycle at 24 ± 1 °C and 55–60% relative humidity. All experimental procedures were conducted in accordance with The Code of Ethics of the World Medical Association (Declaration of Helsinki) for experiments involving humans, EC Directive 86/609/EEC for animal experiments, Uniform Requirements for manuscripts submitted to Biomedical Journals, and approved by the Jiangsu University Committee on Animal Care and Use.

After acclimatization for 3 days, all animals (168) were randomly divided into 6 groups (n = 28/group), including one control group (received clean drinking soybean oil) and five PCB126-treatment groups. The mice were exposed to PCB126 by intragastric administration with five concentrations (0.5, 5, 50, 250, 500 μg/kg body weight). In all treatments, mice were exposed continuously for 3, 5, 7 days. During the exposure period, the bodyweight of mice was measured and recorded.

2.3. Assessment of correlation index

The mice were monitored for health status during the phase of intragastric administration once a day, including the mental state and behavior of mice. At 3, 5 and 7 days during the experiment, the body weight was weighed and recorded, and the rate of weight increase was calculated by the following formula:

$$\Delta M = \frac{M_i - M_0}{M_0}$$

In this formula, ΔM was the rate of weight increasing, M_i was the bodyweight during experiment, M_0 was the bodyweight of the first day of the experiment.

The thymus and spleen of mice were removed aseptically and weighed. The relative weights of organs were calculated as follows:

$$\text{Organ index} = \frac{M_o}{M_b}$$

In the formula, M_o was the organ weight of mice (mg), the M_b was the bodyweight of mice (g).

The blood from eye venous plexus was added into the anticoagulant tube (Violet, EDTA-K2). White blood cells, red blood cells and platelets were assayed by the Mindray BC-2800vet (Mindray, Shenzhen, China) automated haematology analyzer in whole blood specimens collected into EDTA anticoagulant. Serum was separated from the blood by centrifugation. In addition, collected serum was assessed for TNF-α, IFN-γ and IL-2 using ELISA kit (Multi Sciences, China) according to the vendor's protocol.

150–400 mg spleen and thymus tissue were obtained and placed in the amount of saline to prepare the homogenate, respectively. After 3000 r/min centrifuge for 15 min, the malondialdehyde (MDA) content and superoxide dismutase (SOD) activity of the supernatant was determined by MDA and SOD kits.

2.4. Histopathological examination of spleen and thymus

The excised spleen and thymus samples were fixed in paraformaldehyde (4%) for 24 h. Histological staining spleen and thymus paraffin-embedded sections (5 μm) were stained with hematoxylin and eosin (HE) according to the standard procedure. The stained sections were analyzed using the LEICA DM6000 B (LEICA, Germany), and digital images were taken using Image-J 1.8.0.

2.5. ROS examination of spleen

In the present study, DCFH-DA as a fluorescent probe was used to

determine ROS generation. After penetrating cells, DCFH-DA is hydrolyzed into non-fluorescent DCFH by intracellular esterase, and the latter can be quickly oxidized into highly fluorescent DCF when ROS are present. In short, a single-cell suspension was obtained after 200 filter screens and washed twice by DMEM. The cell concentration was adjusted to 2×10^5 with PBS and plated in 96-well plates and then 100 μL DCFH-DA (1:1000 dilutions) was added and incubated at 37 °C for 30 min in the dark. The fluorescence intensities were detected by a fluorescence microplate reader, with excitation and emission wavelengths of 488 and 525 nm, respectively.

2.6. Western blot analysis

The total proteins of Spleen were extracted by use of the Total protein extraction kit. The animal tissues were blended with pre-cooled Lysis buffer and homogenized with ultrasonic homogenizer. Then the homogenate was incubated in an ice water bath for 30 min in the shaker. After being centrifuged at 12000 rpm for 10 min at 4 °C, the supernatant was obtained as the total protein samples of tissues. The protein determination kits of the BCA method were applied to quantitative analysis of the protein samples. Add the standard/samples and 200 μL BCA working liquid mixture into 96-well plates and oscillate to blend them. After incubation at 37 °C for 20–30 min, the absorbance was detected on the microplate reader at 562 nm. Samples were separated by 10% or 12.5% SDS-PAGE, transferred onto nitrocellulose membranes and blocked in 5% nonfat dry milk at 37 °C for 1.5 h. Then, the membranes were incubated with primary antibodies at 4 °C overnight. After washing in TBST three times, the membranes were incubated with appropriate secondary antibodies conjugated to horseradish peroxidase at 37 °C for 2 h. Finally, the proteins were visualized using the ECL system (Beyotime Biotechnology, Shanghai, China).

2.7. Real-time RT-PCR

The mRNA expression of TNF-α, IFN-γ, IL-2, AhR, AhRR, Cyp1a1, Cyp1a2, Cyp1b1, Nrf2 and Keap1 in the splenocyte were detected by real-time RT-PCR, and custom-made primers sequences were shown in Table 1. Briefly, a certain amount of spleen tissue was subjected to Trizol RNA extraction by Trizol reagent (TaKaRa Bio Inc., Japan). The first-strand cDNA was synthesized using an IScript™ cDNA Synthesis Kit. The RT reaction was performed at 25 °C for 5 min, 46 °C for 20 min and 95 °C for 1 min, the obtain cDNA template was then stored at −80 °C for use. Quantitative real-time PCR was performed in triplicate using an ABI 7300 real-time PCR system and an SYBR green PCR master mix reagent kit (TaKaRa). The data were normalized to β-actin and subsequently normalized to an experimental control group ($2^{-\triangle\triangle CT}$ method).

2.8. Statistical analysis

The experimental data are presented as the means ± standard deviation (SD) at least three independent experiments for each condition. Duncan's multiple-range test and one-way analysis of variance (ANOVA) were used for multiple comparisons using SPSS 22 software (SPSS Inc., Chicago, IL, USA). $P^* < 0.05$ was considered to be of statistically significant difference.

Table 2
Effects of PCB126 on the rate of weight growth of mice.

Group	Third day (%)	Fifth day (%)	Seventh day (%)
Blank control	11.91 ± 0.41	27.62 ± 0.68	40.12 ± 1.88
0.5 μg/kg dose	11.53 ± 0.60	23.59 ± 1.51[a]	34.21 ± 1.30[a]
5 μg/kg dose	11.30 ± 0.46	21.50 ± 0.62[a]	31.63 ± 1.46[a]
50 μg/kg dose	10.89 ± 0.66	18.4 ± 1.73[abc]	27.27 ± 0.93[abc]
250 μg/kg dose	10.48 ± 0.46	17.3 ± 1.34[abc]	23.72 ± 1.23[abc]
500 μg/kg dose	9.62 ± 0.82[abc]	15.7 ± 0.70[abc]	20.49 ± 0.64[abcd]

Notes: [a]$p < 0.05$, compared with blank control group; [b]$p < 0.05$, compared with 0.5 μg/kg group; [c]$p < 0.05$, compared with 5 μg/kg group; [d]$p < 0.05$, compared with 50 μg/kg group.

3. Results

3.1. Effect of PCB126 on the growth of mice

The effect of PCB126 on the bodyweight growth rate of mice was presented in Table 2. The body weight gain in all the tested cases revealed no differences before the exposure. During the whole experiment, the bodyweight gain in the control group was significantly increased with the passage of time. However, when compared with the control group, PCB126 exposure significantly inhibited the growth of mice during the exposure period. Specifically, after the end of 5-day exposure, the bodyweight growth rate was significantly inhibited compared with the control group, which revealed that PCB126 could sustainability suppress the growth of bodyweight of mice. Thus, PCB126 is harmful to the growth of mice.

3.2. Effect of PCB126 on organ indexes of mice

The thymus is the primary lymphoid organ that provides a microenvironment that is essential for the development of T cells. The spleen is the largest peripheral immune organ in the body, and it exerts a vital function in local immunity and immune regulation. The relative weight of thymus and spleen were the indicators of both immune organ development and the state of immune in an organism. The relative weight of thymus and spleen in the different treated group were shown in Fig. 1. Compared with the control group, the relative weight of thymus and spleen were significantly decreased ($P < 0.05$) in PCB126 treated group which indicated that exposure to PCB126 can cause atrophy of thymus and spleen and result in toxic effects on the immune system afterwards. Results were similar to the previous investigation (Miyashita et al., 2011). These results showed that PCB126 could

Table 1
List of Real-Time qPCR Primer Sequences.

Gene Name	Forward Primer	Reverse Primer
TNF-α	5′-ATGAGCACAGAAAGCATGATC-3′	5′-TACAGGCTTGTCACTCGAATT-3′
IFN-γ	5′-ATCTGGAGGAACTGGCAAAA-3′	5′-TTCAAGACTTCAAAGAGTCTGAGGTA-3′
IL-2	5′-CCTGAGCAGGATGGAGAATTACA-3′	5′-TCCAGAACATGCCGCAGAG-3′
AhR	5′-AGCCGGTGCAGAAAACAGTAA-3′	5′-AGGCGGTCTAACTCTGTGTTC-3′
AhRR	5′-ACATACGCCGGTAGGAAGAGA-3′	5′-GGTCCAGCTCTGTATTGAGGC-3′
Cyp1a1	5′- GGCCACTTTGACCCTTACAA-3′	5′-CAGGTAACGGAGGACAGGAA-3′
CYP1a2	5′-AGTACATCTCCTTAGCCCCAG-3′	5′-GGTCCGGGTGGATTCTTCAG-3′
CYP1b1	5′-CACCAGCCTTAGTGCAGACAG-3′	5′-GAGGACCACGGTTTCCGTTG-3′
Nrf2	5′- CTGAACTCCTGGACGGGACTA-3′	5′- CGGTGGGTCTCCGTAAATGG-3′
Keap1	5′-TGCCCCTGTGGTCAAAGTG-3′	5′-GGTTCGGTTACCGTCCTGC-3′
β-acting	5′-TGGAATCCTGTGGCATCCATGAAAC-3′	5′-TAAAACGCAGCTCAGTAACAGTCCG-3′

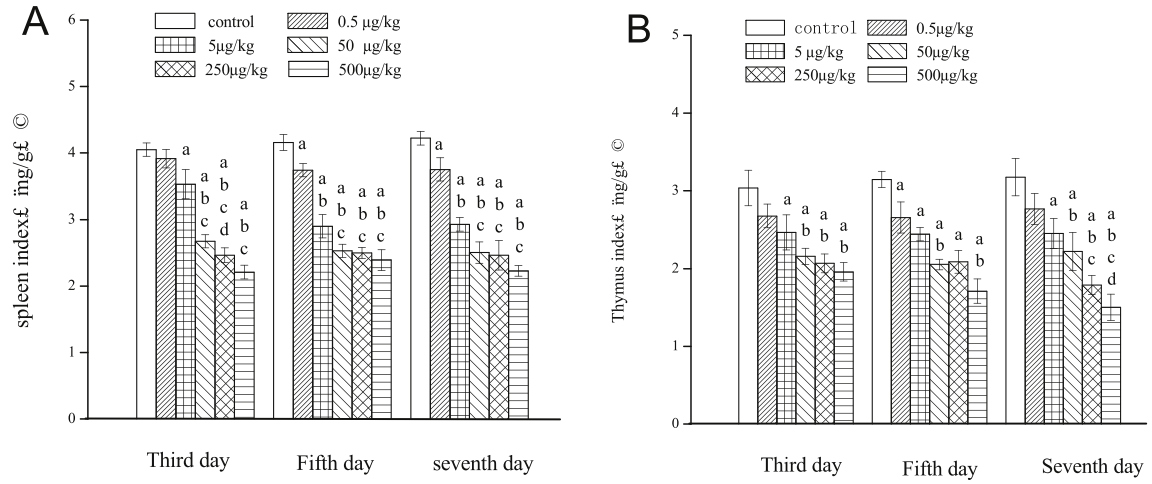

Fig. 1. The effects of PCB 126 treatments for 3 day, 5 day, 7day on splenic organ and thymus organ mass indexes of mice. (A) Effects of PCB126 on splenic indexes of mice. (B) Effects of PCB126 on thymus indexes of mice. Notes: $^{a}p < 0.05$, compared with blank control group; $^{b}p < 0.05$, compared with 0.5 μg/kg group; $^{c}p < 0.05$, compared with 5 μg/kg group; $^{d}p < 0.05$, compared with 50 μg/kg group. Data are expressed as the mean ± SD (n = 5).

impair inherent immunity.

3.3. Effect of PCB126 on SOD activities and MDA levels

SOD is considered as primary antioxidant enzymes, which could catalyze the conversion of O^{2-} to H_2O_2. MDA is the end-product of lipid peroxidation. Both SOD activities and MDA levels can evaluate the redox status of an organism. Levels of SOD and MDA in spleen and thymus of mice treated with PCB126 were summarized in Table 3. There was a significant decrease in the SOD activities of thymus and spleen in PCB126-treated rats. Accompanied with weakening of the antioxidant functions, PCB126 exposure could cause a significant lipid peroxidation to immune cells in spleen and thymus as edvidenced by increasing of MDA levels with cumulative doses. As a result, PCB126 short-term exposure could cause oxidative stress in target organs which is consistent with previous reports (Chen, 2010) and is possibly associated with PCB126 induced toxicity.

3.4. Effects of PCB126 on the levels of TNF-α, IFN-γ and IL-2

The TNF-α is an important component in innate immunity and inflammatory, responses. However, IFN-γ and IL-2 cytokines are essential factors for lymphocyte, proliferation and differentiation. Effects of PCB126 on the levels of TNF-α, IFN-γ and IL-2 in the serum of mice were shown in Fig. 2. The results showed that secretion levels of TNF-α, INF-γ and IL-2 were significantly inhibited in rats serum after exposure PCB126 with dose and time-dependent manner ($P < 0.05$). As a result, one of the immunotoxicity effects of PCB126 on organism is possibly associated with the inhibitory effect of PCB126 on TNF-α, INF-γ and IL-2 cytokines production. From the results of cytokine secretion level, it showed that PCB126 significantly inhibited the secretion of cytokines on the fifth day. Therefore, the effects of PCB126 on the fifth day were selected for the subsequent experiments in the present study.

Table 3
Effects of PCB126 on activities of SOD and levels of MDA in splenic and thymus organs of mice.

Group	Third day (%)	Fifth day (%)	Seventh day (%)
Blank control	11.91 ± 0.41	27.62 ± 0.68	40.12 ± 1.88
0.5 μg/kg dose	11.53 ± 0.60	23.59 ± 1.51^{a}	34.21 ± 1.30^{a}
5 μg/kg dose	11.30 ± 0.46	21.50 ± 0.62^{a}	31.63 ± 1.46^{a}
50 μg/kg dose	10.89 ± 0.66	18.4 ± 1.73^{abc}	27.27 ± 0.93^{abc}
250 μg/kg dose	10.48 ± 0.46	17.3 ± 1.34^{abc}	23.72 ± 1.23^{abc}
500 μg/kg dose	9.62 ± 0.82^{abc}	15.7 ± 0.70^{abc}	20.49 ± 0.64^{abcd}

Notes: $^{a}p < 0.05$, compared with blank control group; $^{b}p < 0.05$, compared with 0.5 μg/kg group; $^{c}p < 0.05$, compared with 5 μg/kg group.

3.5. Effect of PCB126 on haematology

Routine blood tests are one of the critical methods in biology research. Blood is made up of plasma and formed elements, which are white blood cells (WBC), red blood cells (RBC) and platelets (PLT). There are several different types of WBC, including Granulocytes (Gran), lymphocytes (Lymph) and monocytes (Mon). WBC do produce antibodies when encountering a specific antigen, and then bind to the antigen and initiate the foreign cell to phagocytosis. RBC not only has respiratory function, but also plays an important supplement to the WBC immune system. However, platelets have been implicated in inflammatory responses. As shown in Table 4, compared with control group, WBC and PLT were significantly decreased ($P < 0.01$ or $P < 0.05$), whereas RBC was significantly increased in PCB126 exposed groups ($P < 0.01$). Thus, PCB126 could significantly cause the abnormality in hematological parameters.

3.6. Effect of PCB126 on the histopathological changes in thymus

As shown in Fig. 3, the thymus in the experiment group exhibited intact structures with regular morphology and did not display histological changes, and a clear boundary could be observed between the thymus cortex and medulla. The cortex is densely packed with T lymphocytes and epithelial reticular cells, while the medulla has a large number of macrophages, reticulocytes and lymphocytes. The result indicates that PCB126 has only a small effect on the morphology and histology of the thymus.

3.7. Effect of PCB126 on the histopathological changes in spleen

The histological manifestations of spleen in the control and 0.5 μM groups showed normal structure, and there was a clear boundary between the spleen white pulp (WP) and red pulp (RP) (Fig. 4). The WP is densely arranged with splenic corpuscle (SCor) and periarterial lymphatic sheath (PALS), while there was no congestion in red pulp of spleen. In contrast, with the dose exceeds 0.5 μM, PCB126 causes spleen tissue morphological changes, resulting in significant increase in the area of red pulp relative to the white pulp. The amount of macrophages and volume of melano-macrophage centers were increased. In addition, the spleen WP and RP demarcation was blurred, more severe hyperemia

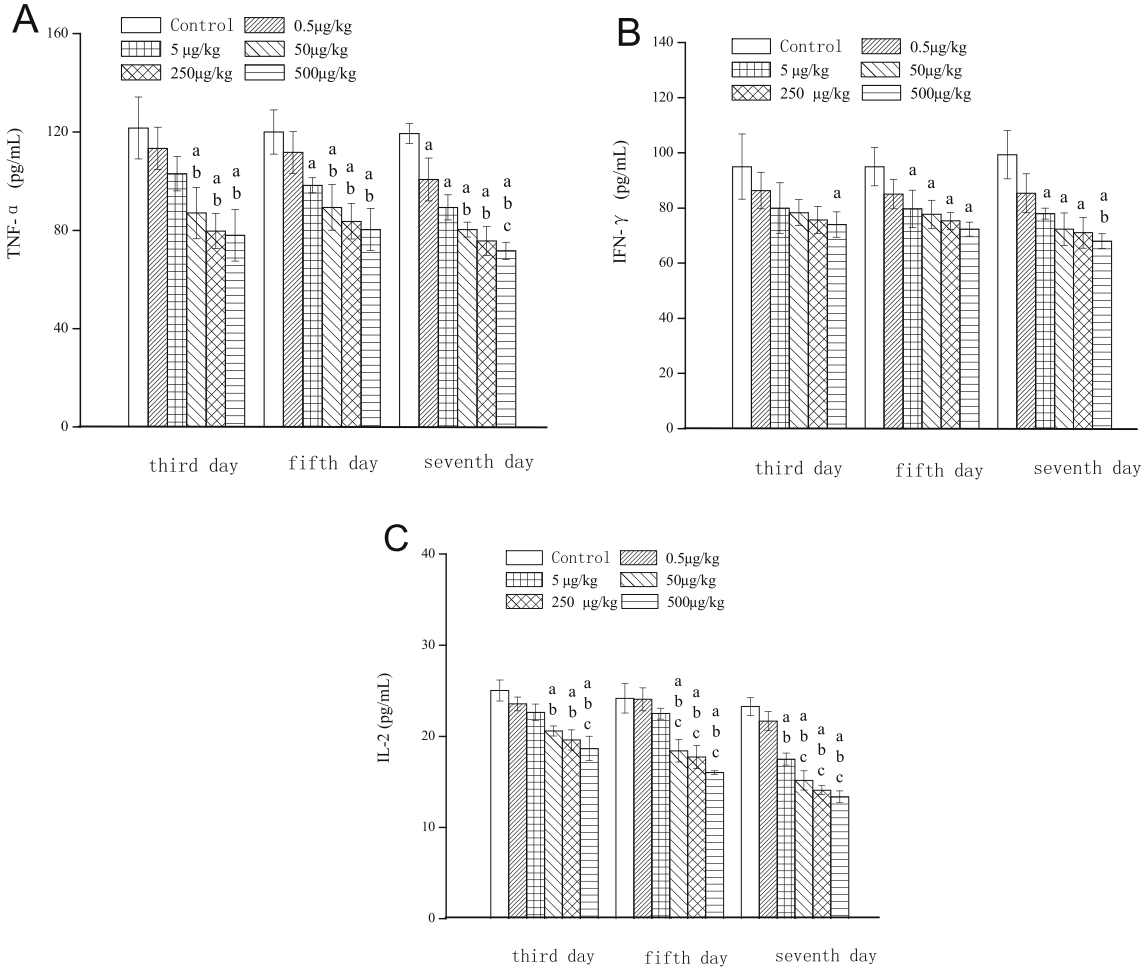

Fig. 2. The effects of PCB126 on the levels of TNF-α, IFN-γ and IL-2 in the serum of mice. (A) Effect of PCB126 on TNF-α level in serum of mice. $^{a}p < 0.05$, compared with blank control group; $^{b}p < 0.05$, compared with 0.5 μg/kg group; $^{c}p < 0.05$, compared with 5 μg/kg group. (B) Effect of PCB126 on IFN-γ level in serum of mice $^{a}p < 0.05$, compared with blank control group; $^{b}p < 0.05$, compared with 0.5 μg/kg group. (C) Effect of PCB126 on IL-2 level in serum of mice. $^{a}p < 0.05$, compared with blank control group; $^{b}p < 0.05$, compared with 0.5 μg/kg group; $^{c}p < 0.05$, compared with 5 μg/kg group.

was induced and the splenic corpuscle with irregular shape was displayed. These results strongly suggested that the treatment of PCB126 resulted in grave tissue damage, further denoting impaired immune function. Therefore, the effects of PCB126 on spleen were selected for the subsequent experiments in the present study.

3.8. Effect of PCB126 on ROS levels

Overproduction of ROS is one of the main manifestations of oxidative stress in cells and tissues. To investigate whether PCB126 can induce spleen cells to release ROS, intracellular ROS levels were detected by DCFH-DA. As shown in Fig. 5, PCB126 induced a remarkable enhancement of ROS generation compared with the control group ($P < 0.01$) in a dose-dependent manner. The results indicated that PCB126 can induce ROS overproduction.

3.9. Effects of PCB126 on mRNA expression of TNF-α, IFN-γ and IL-2

From the results of cytokine secretion level, it showed that PCB126 significantly inhibited the secretion of cytokines on the fifth day. Therefore, the effects of PCB126 on the mRNA expression of TNF-α, IFN-γ and IL-2 in splenic organ on fifth day were determined by RT-PCR in the present study. As shown in Fig. 6, the mRNA levels of TNF-α, IFN-γ and IL-2 significantly decreased with increasing the dose of PCB126

Table 4
Effects of PCB126 on routine blood tests of mice.

Analyte	Control	0.5 μg/kg	5 μg/kg	50 μg/kg	250 μg/kg	500 μg/kg
WBC (10^9/L)	9.41 ± 0.22	7.44 ± 0.31*	7.10 ± 0.28*	4.45 ± 0.21**	6.02 ± 0.17*	6.47 ± 0.11*
Lymph(10^9/L)	5.23 ± 0.18	5.19 ± 0.20	5.03 ± 0.26	2.26 ± 0.10**	4.94 ± 0.15	4.87 ± 0.34
Mon (10^9/L)	0.82 ± 0.05	0.38 ± 0.02*	0.43 ± 0.01*	0.39 ± 0.01*	0.22 ± 0.00**	0.35 ± 0.01**
Gran (10^9/L)	3.49 ± 0.40	2.10 ± 0.18*	1.76 ± 0.14*	1.70 ± 0.22*	0.97 ± 0.12**	1.68 ± 0.08**
RBC (10^{12}/L)	6.87 ± 0.83	7.93 ± 0.92*	8.12 ± 0.68**	7.93 ± 0.39*	7.71 ± 0.31*	8.15 ± 0.40**
HGB (g/L)	130 ± 11	138 ± 14	139 ± 10	138 ± 15	134 ± 12	151 ± 11*
MCHC (g/L)	328 ± 15	327 ± 18	325 ± 27	325 ± 22	334 ± 16	356 ± 19
PLT (10^9/L)	1013 ± 89	821 ± 63*	689 ± 32**	980 ± 26	608 ± 41**	550 ± 31**

Note: $^{*}P < 0.05$, $^{**}P < 0.01$, compared with control group.

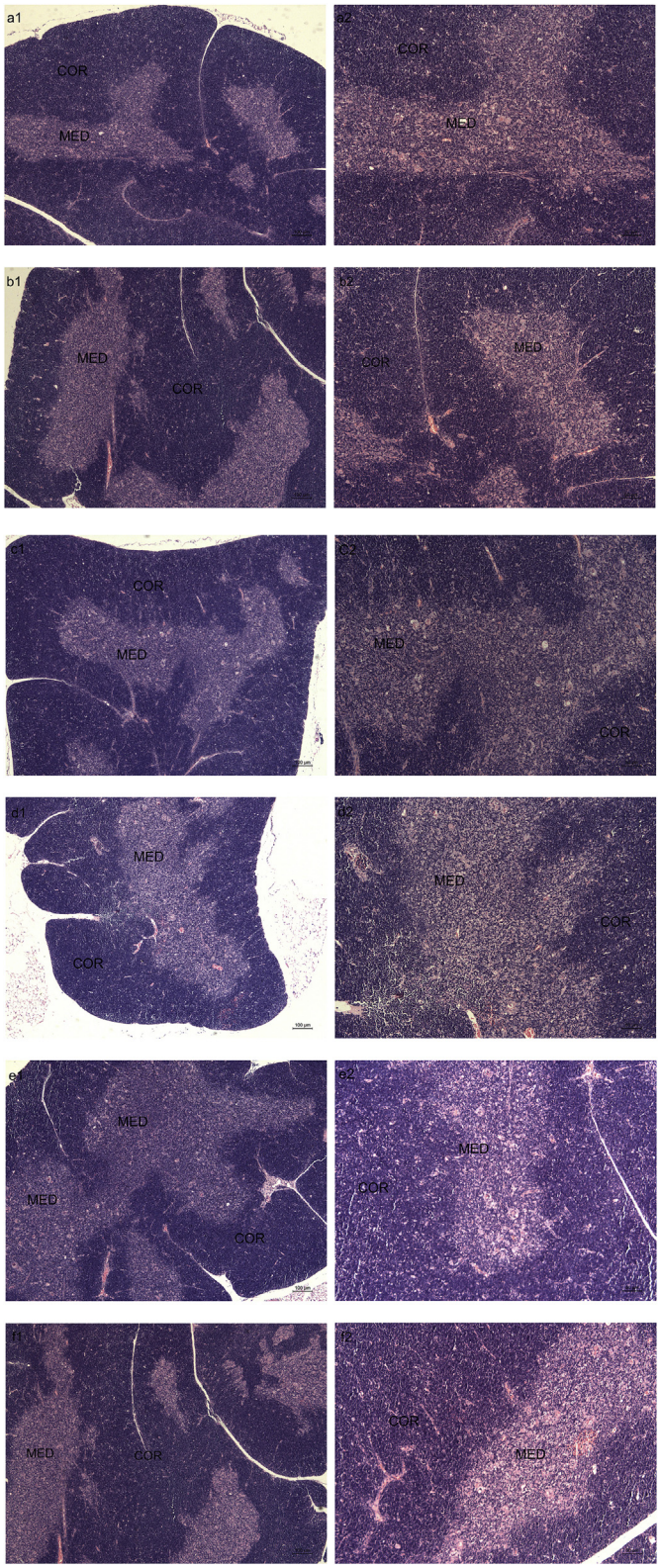

Fig. 3. Effect of PCB126 on the histopathological changes in thymus. (a1) Control, HE, 50 × ; (a2) Control, HE, 100 × ; (b1) 0.5 μg/kg, HE, 50 × ; (b2) 0.5 μg/kg, HE, 100 × ; (c1) 5 μg/kg, HE, 50 × ; (c2) 5 μg/kg, HE, 100 × ; (d1) 50 μg/kg, HE, 50 × ; (d2) 50 μg/kg, HE, 100 × ; (e1) 250 μg/kg, HE, 50 × ; (e2) 250 μg/kg, HE, 100 × ; (f1) 500 μg/kg, HE, 50 × ; (f2) 500 μg/kg, HE, 100 × . MED: Medulla; COR: Cortex.

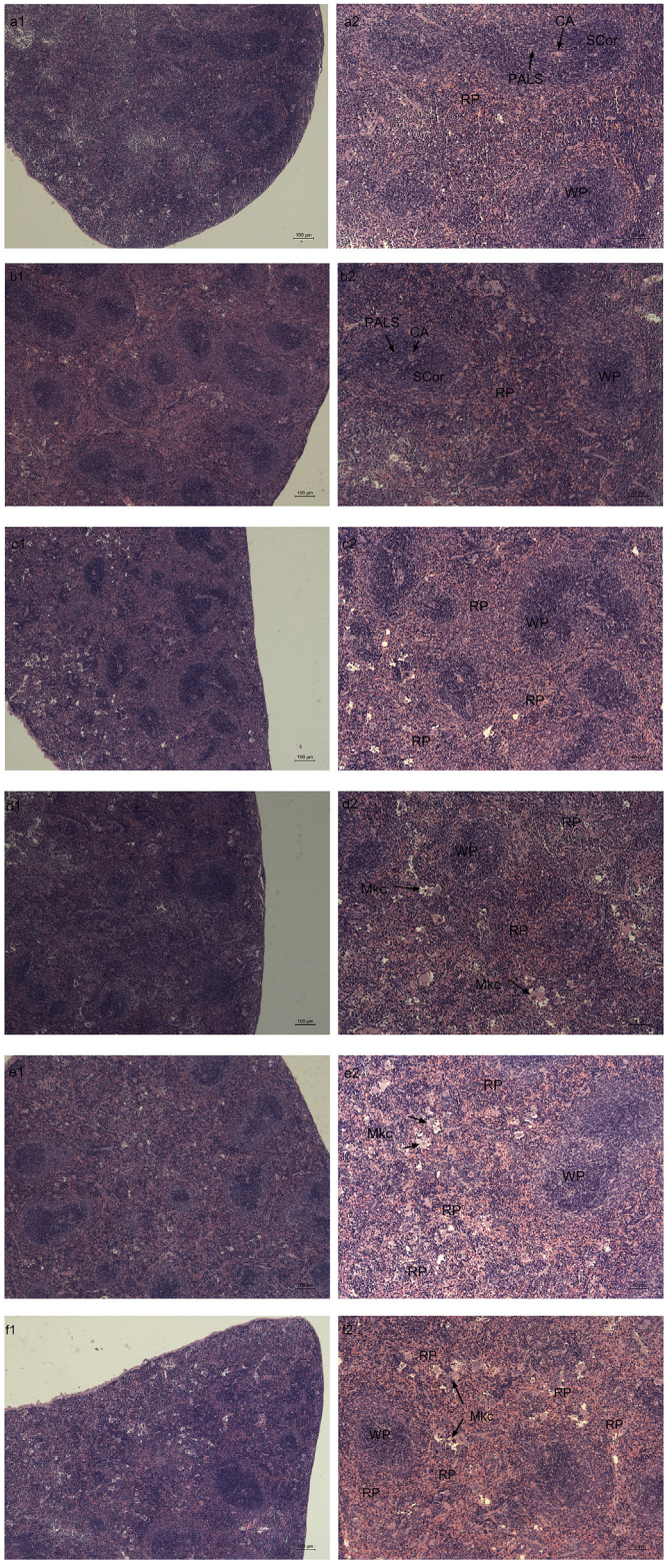

Fig. 4. Effect of PCB126 on the histopathological changes in spleen. (a1) Control, HE, 50 × ; (a2) Control, HE, 100 × ; (b1) 0.5 μg/kg, HE, 50 × ; (b2) 0.5 μg/kg, HE, 100 × ; (c1) 5 μg/kg, HE, 50 × ; (c2) 5 μg/kg, HE, 100 × ; (d1) 50 μg/kg, HE, 50 × ; (d2) 50 μg/kg, HE, 100 × ; (e1) 250 μg/kg, HE, 50 × ; (e2) 250 μg/kg, HE, 100 × ; (f1) 500 μg/kg, HE, 50 × ; (f2) 500 μg/kg, HE, 100 × . RP: Red pulp; WP: White pulp; CA: Central anterry; Mkc: Megakaryocyte; SCor: Splenic corpuscle; PALS: Periarterial lymphatic sheath. (For interpretation of the references to colour in this figure legend, the reader is referred to the Web version of this article.)

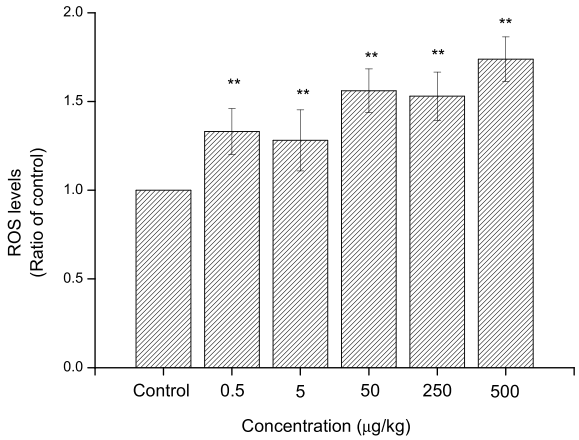

Fig. 5. Variations in ROS of splenocytes treated with PCB126. Control treated with soybean oil. Data are presented as means ± SD (n = 3), *$P < 0.05$, **$p < 0.01$ are compared with control.

($P < 0.05$), which was consisted with the corresponding cytokine levels. Taken together, PCB126 might exert intervention effects of immunotoxicity through elevating the mRNA expressions of TNF-α, IFN-γ and IL-2 in PCB126-treated mice, thus inhibiting the relevant cytokines.

3.10. Effects of PCB126 on mRNA expression of AhR pathway

We validated the expression levels of AhR, AhRR, Cyp1a1, Cp1a2, Cyp1b1 in spleen cell by RT-qPCR. The results demonstrate that PCB126 significantly increased AhR expression ratio to 1.3-fold ($P < 0.05$) at 0.5 μg/kg compared with control group. However, with the dose exceeding 5 μg/kg, the ratio of AhR was significantly decreased, especially at 500 μg/kg (Fig. 7A). AhRR, a negative feedback regulator, at first, the AhRR expression increased with the increase of AhR ($P < 0.01$), especially at lower concentrations (0.5 μg/kg) ($P < 0.01$) (Fig. 7B). Three Cyp1 family enzymes mRNA were increased at the lower and medium dosages of PCB126. when the concentration of PCB126 at 50 μg/kg, mRNA ratio of three Cyp1 family enzymes were up-regulated 5–6 times compared with the control group ($P < 0.01$). In contrast, mRNA of three Cyp1 family enzymes were significantly decreased at a dose of 500 μg/kg ($P < 0.01$).

3.11. Effects of PCB126 on mRNA expression of Nrf2-Keap1

Keap1-Nrf2 is a redox-sensitive signaling pathway that facilitates transcriptional regulation of redox modulatory and cytoprotective genes, which can facilitate the defence against oxidative stress (Kubo et al., 2017). As Fig. 8, at first, both of Nrf2 and Keap1 mRNA ratio significantly increased to 5.2- and 5.2- fold compared with control group at concentration of 50 and 5 μg/kg, respectively. But they was decreased subsequently at 500 μg/kg.

3.12. Effects on apoptosis-related proteins

Apoptosis is mainly mediated by two main pathways, the mitochondrial (intrinsic) apoptotic pathway and the death receptor (extrinsic) pathway. The specific protein expressions of apoptosis were analyzed by western blots and shown in Fig. 9. The toxic mechanism of PCB126 was researched by examining the expression of Bcl-2 and Bax in protein levels. Results showed that Bcl-2 protein level was down-

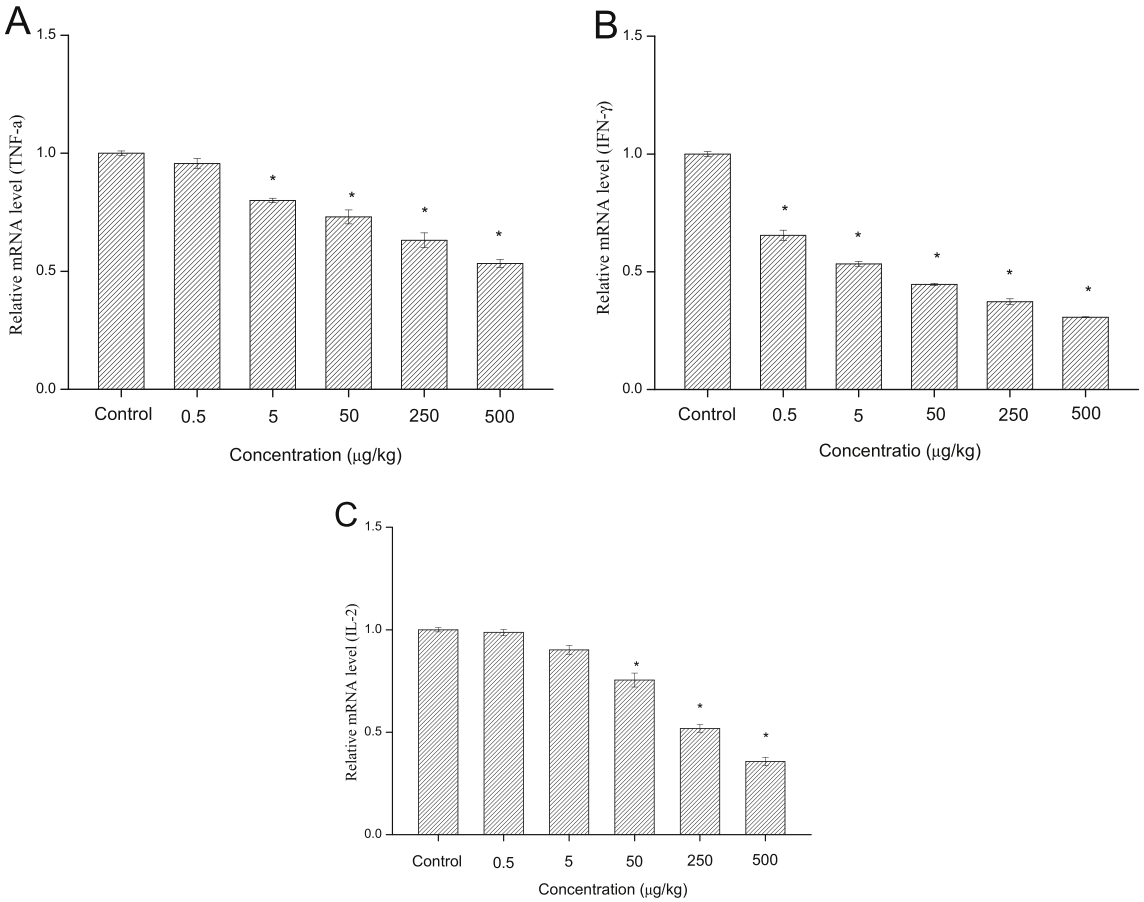

Fig. 6. Effects of PCB126 on (A) TNF-α, (B) IFN-γ and (C) IL-2 mRNA level in the spleen on the fifth day. Results are presented as mean ± SD. ($n = 5$). *$p < 0.05$, and **$p < 0.01$ are compared with control group.

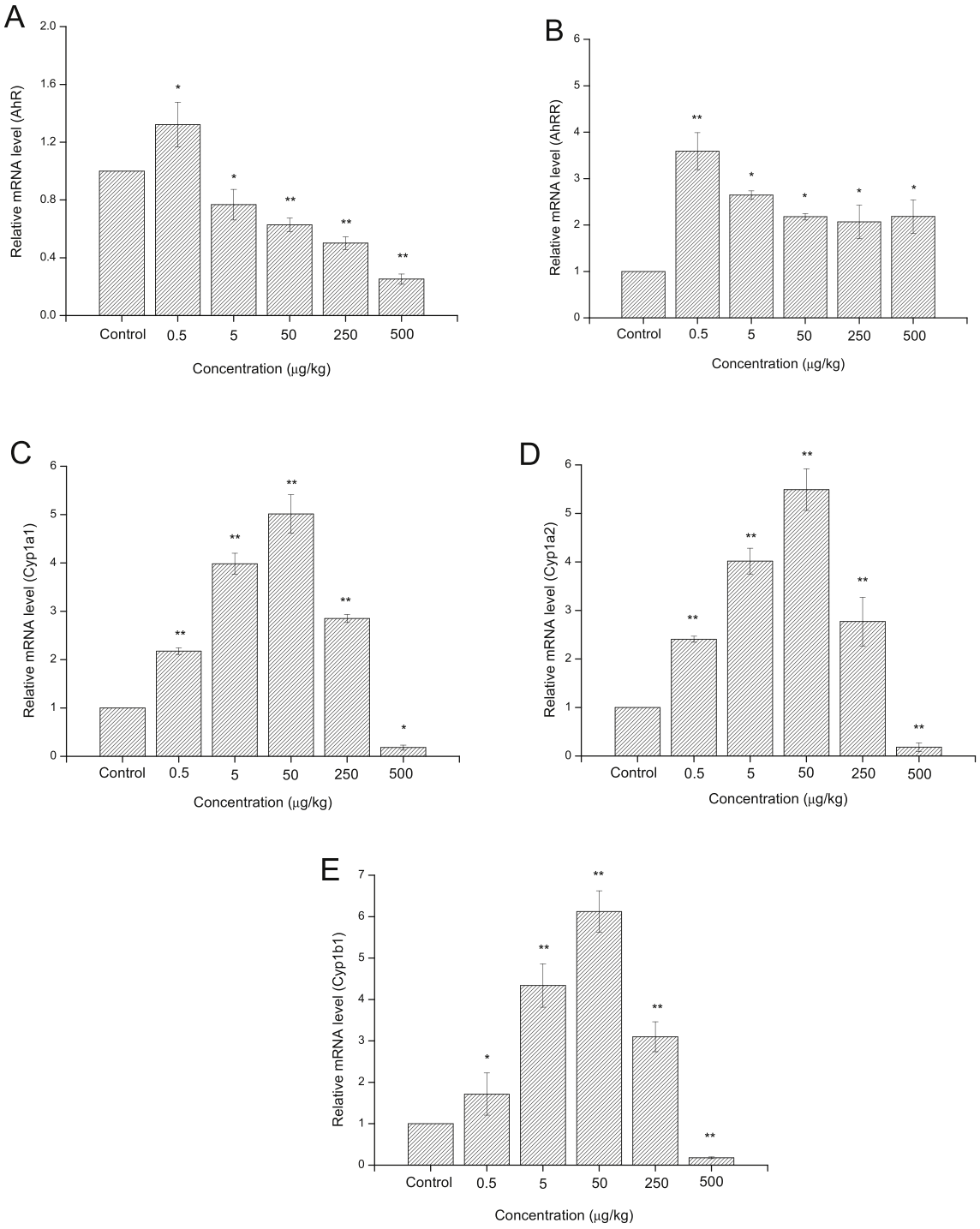

Fig. 7. Effects of PCB126 on (A) AhR, (B) AhRR, (C) Cyp1a1, (D) Cyp1a2 and (E) Cyp1b1 mRNA level in the spleen on the fifth day. Data are presented as mean ± SD (n = 3). *$p < 0.05$, and **$p < 0.01$ are compared with control group.

regulated, while Bax was up-regulated significantly with the increasing concentration of PCB126 compared with the control group ($P < 0.05$) (Fig. 6B–C). With the dose exceeding 50 μg/kg, the protein expression levels of Bcl-2 and Bax were significantly changed. These findings suggested that PCB126 has a potential effect on regulation of the mitochondria apoptosis signal pathway by up-regulating the expression of Bax and down-regulating the Bcl-2 expression dose-dependently.

Caspase family is another initiator and executor of the apoptosis (Brentnall et al., 2013). Among the caspase proteins, caspase-9 and caspase-8 are considered as the essential initiator caspase required for mitochondria-dependent apoptosis signaling (Sitailo et al., 2002). Both caspase-9 and caspase-8 activation could subsequently act on the ultimate enforcer of apoptosis, such as caspase-3. Thus, the expression of caspase-9, caspase-8 and caspase-3 were investigated. Compared with the control group, the expression of caspase-9, caspase-8 and caspase-3 in spleen were increased in dose-dependently (Fig. 7D–F). PCB126 could observably up-regulate the expression of caspase-3 when the dose exceeds 50 μg/kg. PCB126 could significantly up-regulate the expression of caspase-9 and caspase-8 at a high dose. Collectively, PCB126 is capable to elevate the expression of caspases-9, caspase-8 and caspase-3 and then induce splenocyte apoptosis, which indicated that PCB126 might exert an effect on inducing apoptosis of splenocyte through

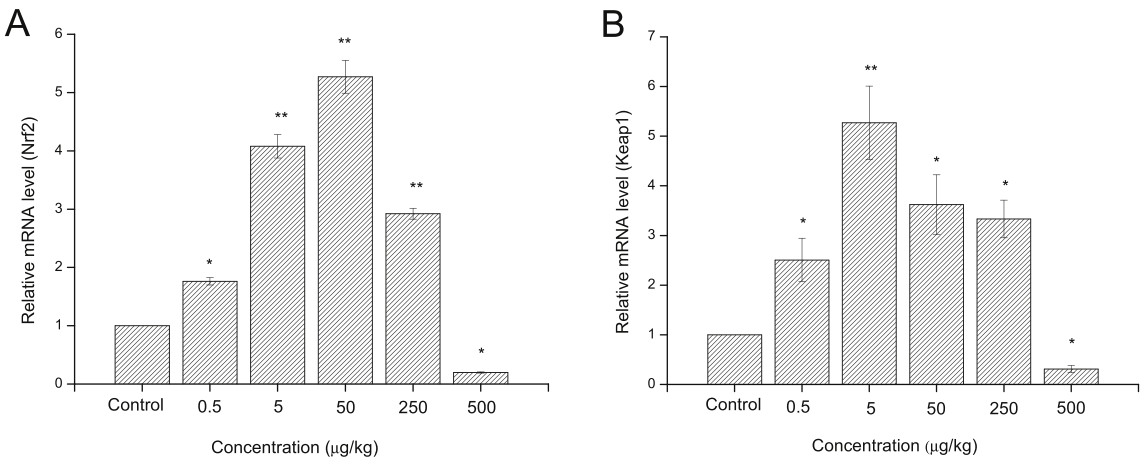

Fig. 8. Effects of PCB126 on (A) Nrf2 and (B) Keap1 mRNA level in the spleen on the fifth day. Data are presented as mean ± SD (n = 3). *$p < 0.05$, and **$p < 0.01$ are compared with control group.

intrinsic and extrinsic apoptosis signal pathway, simultaneously.

4. Discussion

The aryl hydrocarbon receptor (AhR) is an endogenous or exogenous ligand-activated transcription factor. In its inactive state, AhR rests in a cytosolic multiprotein complex. Upon ligand-binding, AhR shuttles in the nucleus dimerizes with AhR nuclear translocator and binds to xenobiotic responsive elements in the enhancer of target genes to initiate their transcription. AhR target genes encode drug-metabolizing enzymes, such as Cyp1a1, Cyp1a2 and Cyp1b1 (Nebert, 2017), which are biological indicators of AhR. Another target is the AhR repressor (AhRR), a negative feedback regulator, which may compete with AhR for both AhR nuclear translocator- and xenobiotic-responsive element-binding (Vogel and Haarmann-Stemmann, 2017). In general, many studies have demonstrated that AhR was activated by exogenous ligand, which resulted in the transcription of Cyp1a1, Cyp1a2 and Cyp1b1. The activation of Cyps induced the generation of ROS, and spurred the emergence of oxidative stress (Knerr et al., 2006). In many cases, irreversible and severe oxidative stress would bring apoptosis to induce toxicity (Lu et al., 2018). From the results, we found that AhR was activated by PCB126 as shown by the increased mRNA expression of Cyp1a1 Cyp1a2 and Cyp1b1 at least at 0.5, 5 and 50 μg/kg. On the one hand, the increase in Cyp1 enzymes mRNA expression is a stress compensation mechanism to metabolize the accumulated ligands, on the other hand, it also leads to the accumulation of ROS in splenocytes, simultaneously. However, the mRNA expression of Cyp1 enzymes was decreased at 250 μg/kg, which may be due to desensitization or decline of AhR mRNA expression and raise of AhRR mRNA expression. Importantly, the mRNA expression of Cyp1 enzymes and AhR were largely decreased at 500 μg/kg, which may be due to overall cellular toxicity hampering the overall mRNA expression at high dosages of PCB126. Additionally, the mRNA expression of Cyp1 enzymes were decreased also may be due to excessive accumulation of ROS (Szychowski et al., 2016). These results further confirmed the cause-and-effect relationship between the AhR pathway and ROS production. Thus, PCB126 up-regulated ROS levels via inducing Cyp1 mRNA expression, which would disturb the redox equilibrium to induce toxicity effect.

As we all know, Keap1-Nrf2 is a redox-sensitive signaling pathway, which would be activated by ROS to up-regulate the genes expression of a series of antioxidant enzymes (SOD, CAT and so on) (Jin et al., 2019). In our study, PCB126 up-regulated the mRNA expression of Nrf2 and keap1 at 0.5–250 μg/kg. However, Nrf2 and keap1 mRNA expression were significantly decreased at 500 μg/kg, which is consistent with previous results, it also may be due to overall cellular toxicity. SOD is considered as primary antioxidant enzymes, which can eliminate O^{2-} and H_2O_2 respectively (Matés et al., 1999). From the results, PCB126 could inhibit the activity of SOD in a dose-dependent manner, it indicates that PCB126 decreases the ability of antioxidant enzymes to eliminate ROS, which is one of the main reasons for ROS accumulation inducing by PCB126. Besides, because of the depletion of SOD activity, the body would regulate the mRNA expression of Nrf2 and Keap1 as the positive feedback to compensate for the body's antioxidant capacity, which is consistent with our results. MDA, an initial indicator of ROS induced damage (Singh et al., 2018), is a small molecular lipid peroxidation product in the body (Vaca et al., 1988). In the present study, the content of MDA was increased by PCB126 in the mice spleen and thymus, which indicate that PCB126 induce production of lipid peroxidation in the immune organ of mice. The above results suggest that PCB126 may induce ROS overproduction by impairing the redox homeostasis, and inducing lipid peroxidation. Thus, the immune function was inhibited by PCB126 through oxidative stress.

Apoptosis is a programmed cell death and an important self-regulatory mechanism for multicellular organisms to maintain homeostasis. Apoptosis is mainly mediated by two main pathways including the mitochondrial (intrinsic) apoptotic pathway and the death receptor (extrinsic) pathway (Pradelli et al., 2010), both of which lead to activate of caspases cascade (Kroemer et al., 2007). It is well known that oxidative stress-induced apoptosis is largely associated with the activation of the intrinsic apoptosis pathways at the level of the mitochondria (Yang et al., 2019). Firstly, ROS disturbs outer membrane permeabilization of mitochondria as the initial factor of apoptosis via activating Bax and inhibiting Bcl-2 expression, afterwards, cytochrome *c* is released into the cytosol (Claro et al., 2014). Then cytochrome *c* activates the initiator caspase-9 to generate the apoptosome (Xu et al., 2019), subsequently it activates the caspase-3 by proteolytic cleavage of redundant part of precursor procaspase-3 (Srinivasula et al., 1998). Finally, the activated caspase-3 would take up the role of executioner caspase to bring about full cellular apoptosis (Xu et al., 2017). In order to get closer mechanistic insight in PCB126-induced apoptosis, the mitochondria-mediated pathway was investigated. The results showed that PCB126 could up-regulate pro-apoptotic proteins (Caspase-3 Caspase-9 and Bax) and down-regulate anti-apoptosis protein (Bcl-2). These results confirmed that PCB126 could induce splenocyte apoptosis via mitochondria-mediated apoptosis pathway. Changes expression of those key proteins demonstrated that the mitochondrial-mediated apoptosis pathway was involved in PCB126-inhibited immune function.

The death receptor pathway is another key regulator of apoptosis. Many studies suggested that environmental pollutants can increase protein expression of Caspase-8 (Ji et al., 2017) by activating receptor pathway on cell membrane (Tanel and Averill-Bates, 2007). And the downstream Caspase-3 is activated subsequently, which induce a series

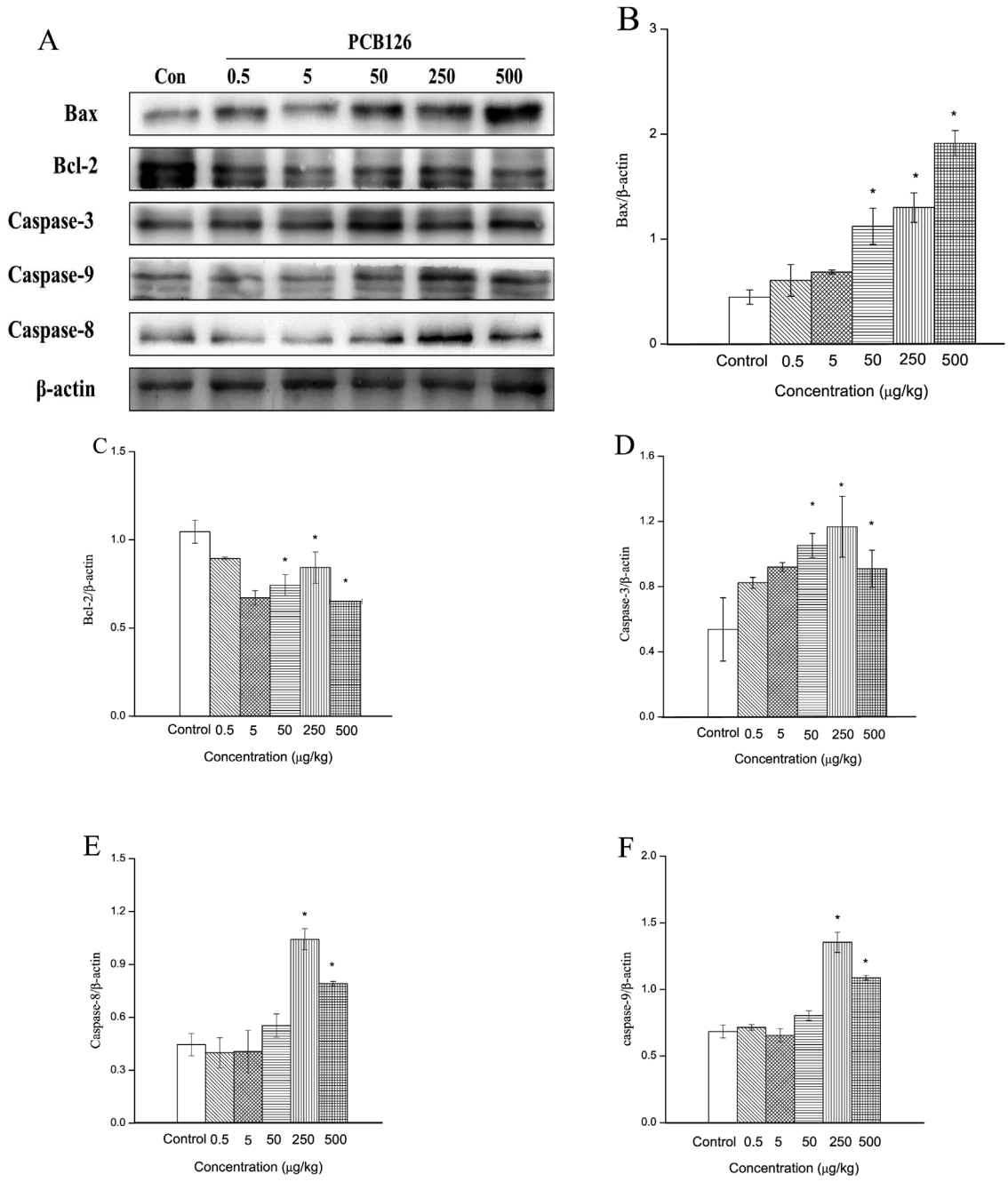

Fig. 9. Effects of PCB126 on Bax、Bcl-2、caspase-3、caspase-8、caspase-9 protein level in the spleen on the fifth day. (A) Western blotting analysis of apoptosis-related protein expression, β-actin was used as the loading control. (B–F) Western blots densitometric analysis. Results are presented as mean ± SD. (n = 5). $^{*}p < 0.05$, and $^{**}p < 0.01$ are compared with control group.

of related cascaded reactions and trigger apoptosis (Xie et al., 2016). The present results indicated that the pro-apoptosis protein of caspase-8 increased remarkably, which revealed that PCB126 could induce splenocyte apoptosis via, death receptor pathway within a certain concentration range.

As we know, cytokines play key roles in the maintenance of the immune response by producing of immune/non-immune cells. Cytokines are classified into pro-inflammatory cytokines, cell-mediated and anti-inflammatory cytokines. IFN-γ, TNF-α and IL-2 belong to the pro-inflammatory cytokines (Liu et al., 2012) and are involved in cellular immunity. Many studies demonstrated that immunosuppression is usually accompanied with the down-regulation of cytokines mRNA expression and secretion levels, such as TNF-α (Liu et al., 2019), IFN-γ (Chae et al., 2019) and IL-2 (Deng et al., 2019a). Consistent with the present results, mRNA expression and secretion levels of TNF-α, IFN-γ and IL-2 were a negative correlation with doses of PCB126 exposure, which implied that PCB126 could cause immunosuppression.

5. Conclusions

This study demonstrated that PCB126 induced immune dysfunction in mice. In summary, PCB126 not only induced growth inhibition, atrophy of thymus and spleen, and severe structural alterations, but also inhibition of cytokines (TNF-α, IFN-γ and IL-2) production by down-regulating the mRNA expressions. Most importantly, the damage of spleen and thymus may at least be partly due to PCB126 inducing oxidative damage via up-regulation MDA contents, down-regulation SOD and interference Nrf2 signaling pathway. In addition, PCB126

induced high reactive oxygen species (ROS) level by disturbing the mRNA expression of AhR and subsequently up-regulating Cyp1 enzymes mRNA expression. The extreme high ROS levels in spleen cells activated mitochondria pathway through elevation Bax/Bcl-2 ratio and protein expression of caspase-9, then results in the activation of caspase-3 to conduct apoptosis. Additionally, PCB126 also upregulate caspase-8 expression mediating spleen cells apoptosis through the extrinsic pathway where cell membrane receptor is involved. The results clearly showed that PCB126 modulated AhR signaling pathway, which interacted with apoptosis and oxidative stress to induce immunotoxicity.

Declaration of Competing interest

The authors declare that they have no known competing financial interests or personal relationships that could have appeared to influence the work reported in this paper.

Acknowledgments

This work was supported by the Natural Science Foundation of China [grant numbers: 21507048]; Jiangsu Provincial Natural Science Fundation of China [grant numbers: BK20150481, BK20160497]; China Prostdoctoral Science Foundation [grant numbers: 2014M551521] and Research Foundation for Advanced Talents in Jiangsu University [grant numbers: 14JDG055].

Appendix A. Supplementary data

Supplementary data to this article can be found online at https://doi.org/10.1016/j.fct.2019.110803.

References

Abella, V., Santoro, A., Scotece, M., Conde, J., López-López, V., Lazzaro, V., Gómez-Reino, J.J., Meli, R., Gualillo, O., 2015. Non-dioxin-like polychlorinated biphenyls (PCB 101, PCB 153 and PCB 180) induce chondrocyte cell death through multiple pathways. Toxicol. Lett. 234, 13–19.

Ampleman, M.D., Andrés, M., Jeanne, D.W., Rawn, D.F.K., Hornbuckle, K.C., Thorne, P.S., 2015. Inhalation and dietary exposure to PCBs in urban and rural cohorts via congener-specific measurements. Environ. Sci. Technol. 49, 1156–1164.

Angerer, J., Ewers, U., Wilhelm, M., 2007. Human biomonitoring: state of the art. Int. J. Hyg Environ. Health 210, 201–228.

Baqar, M., Sadef, Y., Ahmad, S.R., Mahmood, A., Qadir, A., Aslam, I., Li, J., Zhang, G., 2017. Occurrence, ecological risk assessment, and spatio-temporal variation of polychlorinated biphenyls (PCBs) in water and sediments along River Ravi and its northern tributaries, Pakistan. Environ. Sci. Pollut. Res. 24, 1–18.

Bertocchi, L., Ghidini, S., Fedrizzi, G., Lorenzi, V., 2015. Case-study and risk management of dioxins and PCBs bovine milk contaminations in a high industrialized area in Northern Italy. Environ. Sci. Pollut. Res. 22, 9775–9785.

Bodin, N., Tapie, N., Le Ménach, K., Chassot, E., Elie, P., Rochard, E., Budzinski, H., 2014. PCB contamination in fish community from the Gironde Estuary (France): blast from the past. Chemosphere 98, 66–72.

Brentnall, M., Rodriguezmenocal, L., Guevara, R.L.D., Cepero, E., Boise, L.H., 2013. Caspase-9, caspase-3 and caspase-7 have distinct roles during intrinsic apoptosis. BMC Cell Biol. 14 32-32.

Chae, J.S., Shin, H., Song, Y., Kang, H., Yeom, C.-H., Lee, S., Choi, Y.S., 2019. Yeast (1→3)-(1→6)-β-d-glucan alleviates immunosuppression in gemcitabine-treated mice. Int. J. Biol. Macromol. 136, 1169–1175.

Chen, F., 2010. Induction of oxidative stress and cytotoxicity by PCB126 in JEG-3 human choriocarcinoma cells. J. Environ. Sci. Health Part A 45, 932–937.

Chen, Y., Liu, Y., 2019. Non-coplanar and coplanar polychlorinated biphenyls potentiate genotoxicity of aflatoxin B1 in a human hepatocyte line by enhancing CYP1A2 and CYP3A4 expression. Environ. Pollut. 246, 945–954.

Chu, C.-P., Wu, S.-W., Huang, Y.-J., Chiang, M.-C., Hsieh, S.-T., Guo, Y.L., 2019. Neuroimaging signatures of brain plasticity in adults with prenatal exposure to polychlorinated biphenyls: altered functional connectivity on functional MRI. Environ. Pollut. 250, 960–968.

Claro, S., Oshiro, M.E.M., Mortara, R.A., Paredes-Gamero, E.J., Pereira, G.J.S., Smaili, S.S., Ferreira, A.T., 2014. γ-Rays-generated ROS induce apoptosis via mitochondrial and cell cycle alteration in smooth muscle cells. Int. J. Radiat. Biol. 90, 914–927.

Deng, N., Li, M., Shen, D., He, Q., Sun, W., Liu, M., Liu, Y., Zhou, Y., Zheng, J., Shen, F., 2019a. LRP1 receptor-mediated immunosuppression of α-MMC on monocytes. Int. Immunopharmacol. 70, 80–87.

Deng, P., Barney, J., Petriello, M.C., Morris, A.J., Wahlang, B., Hennig, B., 2019b. Hepatic metabolomics reveals that liver injury increases PCB 126-induced oxidative stress and metabolic dysfunction. Chemosphere 217, 140–149.

Falandysz, J., Smith, F., Panton, S., Fernandes, A.R., 2019. A retrospective investigation into the occurrence and human exposure to polychlorinated naphthalenes (PCNs), dibenzo-p-dioxins and furans (PCDD/Fs) and PCBs through cod liver products (1972–2017). Chemosphere 231, 240–248.

Fiandanese, N., Borromeo, V., Berrini, A., Fischer, B., Schaedlich, K., Schmidt, J.-S., Secchi, C., Pocar, P., 2016. Maternal exposure to a mixture of di (2-ethylhexyl) phthalate (DEHP) and polychlorinated biphenyls (PCBs) causes reproductive dysfunction in adult male mouse offspring. Reprod. Toxicol. 65, 123–132.

Fischer, C., Fredriksson, A., Eriksson, P., 2008. Neonatal co-exposure to low doses of an ortho-PCB (PCB 153) and methyl mercury exacerbate defective developmental neurobehavior in mice. Toxicology 244, 157–165.

Gaum, P.M., Lang, J., Esser, A., Schettgen, T., Neulen, J., Kraus, T., Gube, M., 2016. Exposure to polychlorinated biphenyls and the thyroid gland–examining and discussing possible longitudinal health effects in humans. Environ. Res. 148, 112–121.

Hoang, T.T., Traag, W.A., Murk, A.J., Hoogenboom, R.L., 2014. Levels of polychlorinated dibenzo-p-dioxins, dibenzofurans (PCDD/Fs) and dioxin-like PCBs in free range eggs from Vietnam, including potential health risks. Chemosphere 114, 268–274.

Ingelido, A.M., Abate, V., Abballe, A., Albano, F.L., Battista, T., Carraro, V., Conversano, M., Corvetti, R., De Luca, S., Franchini, S., 2017. Concentrations of polychlorinated dibenzodioxins, polychlorodibenzofurans, and polychlorobiphenyls in women of reproductive age in Italy: a human biomonitoring study. Int. J. Hyg Environ. Health 220, 378–386.

Jeon, Y.J., Youk, E.S., Sang, H.L., Suh, J., Yong, J.N., Kim, H.M., 2002. Polychlorinated biphenyl-induced apoptosis of murine spleen cells is aryl hydrocarbon receptor independent but caspases dependent. Toxicol. Appl. Pharmacol. 181, 69–78.

Ji, Y., Yu, M., Qi, Z., Cui, D., Xin, G., Wang, B., Jia, W., Chang, L., 2017. Study on apoptosis effect of human breast cancer cell MCF-7 induced by lycorine hydrochloride via death receptor pathway. Saudi Pharm. J. 25, 633.

Jin, L., Ni, J., Tao, Y., Weng, X., Zhu, Y., Yan, J., Hu, B., 2019. N-acetylcysteine attenuates PM2. 5-induced apoptosis by ROS-mediated Nrf2 pathway in human embryonic stem cells. Sci. Total Environ. 666, 713–720.

Knerr, S., Schaefer, J., Both, S., Mally, A., Dekant, W., Schrenk, D., 2006. 2, 3, 7, 8-Tetrachlorodibenzo-p-dioxin induced cytochrome P450s alter the formation of reactive oxygen species in liver cells. Mol. Nutr. Food Res. 50, 378–384.

Kroemer, G., Galluzzi, L., Brenner, C., 2007. Mitochondrial membrane permeabilization in cell death. Physiol. Rev. 87, 99–163.

Kubo, E., Chhunchha, B., Singh, P., Sasaki, H., Singh, D.P., 2017. Sulforaphane reactivates cellular antioxidant defense by inducing Nrf2/ARE/Prdx6 activity during aging and oxidative stress. Sci. Rep. 7, 14130.

Kuiper, J., Moran, M., Cetkovic-Cvrlje, M., 2016. Exposure to polychlorinated biphenyl-153 decreases incidence of autoimmune type 1 diabetes in non-obese diabetic mice. J. Immunotoxicol. 13, 850–860.

Liu, H., Zhang, Y., Li, M., Luo, P., 2019. Beneficial effect of Sepia esculenta ink polysaccharide on cyclophosphamide-induced immunosuppression and ovarian failure in mice. Int. J. Biol. Macromol. 140, 1098–1105.

Liu, Y., Ho, R.C., Mak, A., 2012. Interleukin (IL)-6, tumour necrosis factor alpha (TNF-α) and soluble interleukin-2 receptors (sIL-2R) are elevated in patients with major depressive disorder: a meta-analysis and meta-regression. J. Affect. Disord. 139, 230–239.

Lu, Q., Zhou, Y., Hao, M., Li, C., Wang, J., Shu, F., Du, L., Zhu, X., Zhang, Q., Yin, X., 2018. The mTOR promotes oxidative stress-induced apoptosis of mesangial cells in diabetic nephropathy. Mol. Cell. Endocrinol. 473, 31–43.

Maranghi, F., Tassinari, R., Moracci, G., Altieri, I., Rasinger, J., Carroll, T., Hogstrand, C., Lundebye, A.-K., Mantovani, A., 2013. Dietary exposure of juvenile female mice to polyhalogenated seafood contaminants (HBCD, BDE-47, PCB-153, TCDD): comparative assessment of effects in potential target tissues. Food Chem. Toxicol. 56, 443–449.

Marlowe, J.L., Fan, Y., Chang, X., Peng, L., Knudsen, E.S., Xia, Y., Puga, A., 2008. The aryl hydrocarbon receptor binds to E2F1 and inhibits E2F1-induced apoptosis. Mol. Biol. Cell 19, 3263–3271.

Matés, J.M., Pérez-Gómez, C., De Castro, I.N., 1999. Antioxidant enzymes and human diseases. Clin. Biochem. 32, 595–603.

Mertes, F., Mumbo, J., Pandelova, M., Bernhöft, S., Corsten, C., Henkelmann, B., Bussian, B.M., Schramm, K.-W., 2018. Comparative study of dioxin contamination from forest soil samples (BZE II) by mass spectrometry and EROD bioassay. Environ. Sci. Pollut. Res. 25, 3977–3984.

Miyashita, C., Sasaki, S., Saijo, Y., Washino, N., Okada, E., Kobayashi, S., Konishi, K., Kajiwara, J., Todaka, T., Kishi, R., 2011. Effects of prenatal exposure to dioxin-like compounds on allergies and infections during infancy. Environ. Res. 111, 551–558.

Moraleshernández, A., Corralesredondo, M., Marcosmerino, J.M., Gonzálezrico, F.J., Sánchezmartín, F.J., Merino, J.M., 2016. AhR-dependent 2,3,7,8-tetrachlorodibenzo-p-dioxin toxicity in human neuronal cell line SHSY5Y. Neurotoxicology (Little Rock) 56, 55–63.

Nebert, D.W., 2017. Aryl hydrocarbon receptor (AHR): "pioneer member" of the basic-helix/loop/helix per-Arnt-sim (bHLH/PAS) family of "sensors" of foreign and endogenous signals. Prog. Lipid Res. 67, 38–57.

Pirard, C., Eppe, G., Massart, A.C., Fierens, S., De, P.E., Focant, J.F., 2005. Environmental and human impact of an old-timer incinerator in terms of dioxin and PCB level: a case study. Environ. Sci. Technol. 39, 4721–4728.

Pradelli, L.A., Bénéteau, M., Ricci, J.E., 2010. Mitochondrial control of caspase-dependent and -independent cell death. Cell. Mol. Life Sci. 67, 1589–1597.

Rusin, M., Dziubanek, G., Marchwińska-Wyrwał, E., Ćwieląg-Drabek, M., Razzaghi, M., Piekut, A., 2019. PCDDs, PCDFs and PCBs in locally produced foods as health risk factors in Silesia Province, Poland. Ecotoxicol. Environ. Saf. 172, 128–135.

Santoro, A., Ferrante, M.C., Di Guida, F., Pirozzi, C., Lama, A., Simeoli, R., Clausi, M.T., Monnolo, A., Mollica, M.P., Mattace Raso, G., 2015. Polychlorinated biphenyls (PCB 101, 153, and 180) impair murine macrophage responsiveness to lipopolysaccharide: involvement of NF-κB pathway. Toxicol. Sci. 147, 255–269.

Singh, C., Prakash, C., Tiwari, K.N., Mishra, S.K., Kumar, V., 2018. Premna integrifolia ameliorates cyclophosphamide-induced hepatotoxicity by modulation of oxidative stress and apoptosis. Biomed. Pharmacother. 107, 634–643.

Sitailo, L.A., Tibudan, S.S., Denning, M.F., 2002. Activation of caspase-9 is required for UV-induced apoptosis of human keratinocytes. J. Biol. Chem. 277, 19346–19352.

Srinivasula, S.M., Ahmad, M., Fernandes-Alnemri, T., Alnemri, E.S., 1998. Autoactivation of procaspase-9 by apaf-1-mediated oligomerization. Mol. Cell 1, 949–957.

Stølevik, S.B., Nygaard, U.C., Namork, E., Haugen, M., Meltzer, H.M., Alexander, J., Knutsen, H.K., Aaberge, I., Vainio, K., van Loveren, H., 2013. Prenatal exposure to polychlorinated biphenyls and dioxins from the maternal diet may be associated with immunosuppressive effects that persist into early childhood. Food Chem. Toxicol. 51, 165–172.

Syed, J.H., Malik, R.N., Li, J., Chaemfa, C., Zhang, G., Jones, K.C., 2014. Status, distribution and ecological risk of organochlorines (OCs) in the surface sediments from the Ravi River, Pakistan. Sci. Total Environ. 472, 204–211.

Szychowski, K.A., Wnuk, A., Kajta, M., Wójtowicz, A.K., 2016. Triclosan activates aryl hydrocarbon receptor (AhR)-dependent apoptosis and affects Cyp1a1 and Cyp1b1 expression in mouse neocortical neurons. Environ. Res. 151, 106–114.

Takahashi, S., Tue, N.M., Takayanagi, C., Suzuki, G., Matsukami, H., Viet, P.H., Kunisue, T., Tanabe, S., 2017. PCBs, PBDEs and dioxin-related compounds in floor dust from an informal end-of-life vehicle recycling site in northern Vietnam: contamination levels and implications for human exposure. J. Mater. Cycles Waste Manag. 19, 1333–1341.

Tanel, A., Averill-Bates, D.A., 2007. Activation of the death receptor pathway of apoptosis by the aldehyde acrolein. Free Radical Biol. Med. 42, 798–810.

Tsuji, G., Takahara, M., Uchi, H., Matsuda, T., Chiba, T., Takeuchi, S., Yasukawa, F., Moroi, Y., Furue, M., 2012. Identification of ketoconazole as an AhR-Nrf2 activator in cultured human keratinocytes: the basis of its anti-inflammatory effect. J. Investig. Dermatol. 132, 59–68.

Vaca, C.E., Wilhelm, J., Harms-Ringdahl, M., 1988. Interaction of lipid peroxidation products with DNA. Rev. Mutat. Res. 195, 137–149.

Vogel, C.F., Haarmann-Stemmann, T., 2017. The aryl hydrocarbon receptor repressor–more than a simple feedback inhibitor of AhR signaling: clues for its role in inflammation and cancer. Curr. Opin. Toxicol. 2, 109–119.

Wang, C., Petriello, M.C., Zhu, B., Hennig, B., 2019. PCB 126 induces monocyte/macrophage polarization and inflammation through AhR and NF-κB pathways. Toxicol. Appl. Pharmacol. 367, 71–81.

Wang, M., Hou, M., Zhao, K., Li, H., Han, Y., Liao, X., Chen, X., Liu, W., 2016. Removal of polychlorinated biphenyls by desulfurization and emissions of polychlorinated biphenyls from sintering plants. Environ. Sci. Pollut. Res. Int. 23, 7369–7375.

Weisglas-Kuperus, N., Patandin, S., Berbers, G.A., Sas, T.C., Mulder, P.G., Sauer, P.J., Hooijkaas, H., 2000. Immunologic effects of background exposure to polychlorinated biphenyls and dioxins in Dutch preschool children. Environ. Health Perspect. 108, 1203–1207.

Xie, H., Huang, H., He, W., Fu, Z., Luo, C., Ashraf, M.A., 2016. Research on in vitro release of Isoniazid (INH) super paramagnetic microspheres in different magnetic fields. Pak. J. Pharm. Sci. 29, 2207–2212.

Xu, F., Gao, X., Li, H., Xu, S., Li, X., Hu, X., Li, Z., Xu, J., Hua, H., Li, D., 2019. Hydrogen sulfide releasing enmein-type diterpenoid derivatives as apoptosis inducers through mitochondria-related pathways. Bioorg. Chem. 82, 192–203.

Xu, S., Yao, H., Luo, S., Zhang, Y.-K., Yang, D.-H., Li, D., Wang, G., Hu, M., Qiu, Y., Wu, X., 2017. A novel potent anticancer compound optimized from a natural oridonin scaffold induces apoptosis and cell cycle arrest through the mitochondrial pathway. J. Med. Chem. 60, 1449–1468.

Yang, F., Pei, R., Zhang, Z., Liao, J., Yu, W., Qiao, N., Han, Q., Li, Y., Hu, L., Guo, J., 2019. Copper induces oxidative stress and apoptosis through mitochondria-mediated pathway in chicken hepatocytes. Toxicol. In Vitro 54, 310–316.

Zhang, L., Yin, S., Wang, X., Li, J., Zhao, Y., Li, X., Shen, H., Wu, Y., 2015. Assessment of dietary intake of polychlorinated dibenzo-p-dioxins and dibenzofurans and dioxin-like polychlorinated biphenyls from the Chinese Total Diet Study in 2011. Chemosphere 137, 178–184.